

# The effect of spatially correlated disorder on the hole transport in disordered semiconducting polymers

J. Y. LIU, L. ZHANG, S. J. GUO, L. G. WANG\*

*School of Electrical Engineering and Automation, Henan Polytechnic University, Jiaozuo, 454000, People's Republic of China*

Recently, it has been demonstrated that the presence of spatial correlation between the disordered transport site energies in organic semiconductors is known to affect the charge carrier mobility. However, it is not established whether the site energies are actually spatially correlated in relevant materials. In this paper, we study the hole transport in the poly (2-methoxy-5-(3', 7'-dimethyloctyloxy)-p-phenylene vinylene) (OC<sub>1</sub>C<sub>10</sub>-PPV) and an analysis of the temperature dependent and layer thickness dependent current density versus voltage ( $J - V$ ) characteristics is proposed. Consistent descriptions with equal quality are obtained by using our recently introduced improved extended Gaussian disorder model (IEGDM) and the extended correlated disorder model (ECDM), within which spatial correlation between the site energies is absent and is included, respectively. We present a comparison of the model parameters between the analysis of the  $J - V$  characteristics using the IEGDM and the ECDM. It is found that the intersite distance obtained using the IEGDM is more realistic than the value obtained in the case of the ECDM. We view this as an indication that spatial correlation between the site energies is absent or plays a minor role in disordered semiconducting polymers.

(Received November 18, 2018; accepted June 14, 2019)

*Keywords:* Hole Transport, Spatially correlated disorder, Intersite distance, Conjugated polymers

## 1. Introduction

In recent decades, organic electronics is an emerging field where organic semiconducting materials are optimized for various applications, such as organic light-emitting diodes (OLEDs) [1, 2], organic field-effect transistors (OFETs) [3, 4], and organic solar cells (OSCs) [5, 6]. The performance of these solution-processed, light-weight, and potentially cost-effective materials heavily relies on their charge carrier mobility. For typical organic semiconductors around room temperature the mobility is dominated by disorder and reflects the ability of the charge carriers to hop between molecular sites in a density of localized states that is broadened by energetic and spatial disorder. Many investigations have demonstrated that the most important parameter controlling the organic electronic devices performance is the mobility, which quantifies how easily charge carriers move when an electric field is applied. Consequently, the mobility is a valuable figure of merit to characterize the underlying physical mechanisms of the charge transport.

It is well known that understanding the dependence of the mobility on the various parameters of the system is crucial to develop a predictive organic electronic device model. In past decades, the dependence of the mobility on the temperature and electric field has been extensively investigated. In the early modeling introduced by Bässler

et al. [7, 8], the random energies were described by a Gaussian density of states (DOS), leading to the Gaussian disorder model (GDM). In this model, it is assumed that there is no spatial correlation between the site energies. Alternatively, it was suggested that the presence of dipole moments in organic semiconductors can give rise to spatial correlation between the site energies [9, 10], leading to the correlated disorder model (CDM). Later, it was realized that, apart from the dependence of the mobility on the temperature and electric field, there is a strong dependence on the charge-carrier density [11–15], giving rise to the extended versions of the GDM and the CDM, the EGDM and the ECDM [16, 17], respectively. However, it should be noted that the EGDM, having a non-Arrhenius temperature dependence  $\ln(\mu) \propto 1/T^2$ , can only well describe the charge transport at low carrier densities. In order to better describe the charge transport, we proposed an improved model in which the mobility depends on the temperature, electric field, and carrier density based on both the non-Arrhenius temperature dependence and Arrhenius temperature dependence  $\ln(\mu) \propto 1/T$  [18], which is known as the improved extended Gaussian disorder model (IEGDM). It has been demonstrated that the improved mobility model can rather well describe the charge transport in various organic materials [19-21].

The key issue in both the GDM and the CDM is the role of the energetic disorder of the states in between

which the charge carrier hopping takes place, assuming a Gaussian density of state (DOS) with random and spatially correlated energetic disorder, respectively. In several studies, it has been revealed that equally good descriptions of the calculated and measured current density versus voltage ( $J-V$ ) curves of the charge transport in organic semiconductors could be obtained from the GDM and the CDM [22-25]. The question now arises whether a successful analysis of the  $J-V$  characteristics of a certain material using the GDM or the CDM would convincingly proof that the disorder is random or correlated, respectively. In this paper, the possible presence of spatially correlated disorder and the  $J-V$  characteristics of the hole transport for an amorphous conjugated polymer poly (2-methoxy-5-(3', 7'-dimethyloctyloxy)-p-phenylene vinylene) (OC<sub>1</sub>C<sub>10</sub>-PPV) are investigated. It is found that equally good descriptions of the layer thickness dependent and temperature dependent  $J-V$  characteristics of OC<sub>1</sub>C<sub>10</sub>-PPV hole-only devices can be obtained within the IEGDM and the ECDM, but a more realistic value of the intersite distance is obtained within the IEGDM than within the ECDM. This is an indication that in OC<sub>1</sub>C<sub>10</sub>-PPV spatially correlation between the site energies is absent or plays a minor role.

## 2. Models and methods

The improved mobility model (IEGDM) in which the mobility  $\mu$  depends on the temperature  $T$ , electric field  $E$ , and carrier density  $p$  based on both the non-Arrhenius temperature dependence and Arrhenius temperature dependence can be described as follows [18]:

$$\mu(T, p, E) = \mu(T, p)^{g(T, E)} \exp[c_4(g(T, E) - 1)], \quad (1)$$

$$\mu(T, p) = \mu_0(T) \exp\left[\frac{1}{2}(\hat{\sigma}^2 - \hat{\sigma})(2pa^3)^\delta\right], \quad (2a)$$

$$\mu_0(T) = \mu_0 c_1 \exp(c_2 \hat{\sigma} - c_3 \hat{\sigma}^2), \quad (2b)$$

$$\delta \equiv 2 \frac{\ln(\hat{\sigma}^2 - \hat{\sigma}) - \ln(\ln 4)}{\hat{\sigma}^2}, \quad \mu_0 \equiv \frac{a^2 v_0 e}{\sigma}, \quad (2c)$$

$$g(T, E) = [1 + c_5 (Eea/\sigma)^2]^{-1/2}, \quad (3)$$

with  $c_1 = 0.48 \times 10^{-9}$ ,  $c_2 = 0.80$ , and  $c_3 = 0.52$ , where  $\mu_0(T)$  is the mobility in the limit of zero carrier density and zero electric field,  $\hat{\sigma} \equiv \sigma/k_B T$  and  $\sigma$  is the width of the Gaussian density of states (DOS),  $a$  is the intersite distance,  $v_0$  is the attempt frequency,  $c_4$  and  $c_5$  are weak density dependent parameters, given by

$$c_4 = d_1 + d_2 \ln(pa^3) \quad (4a)$$

$$c_5 = 1.16 + 0.09 \ln(pa^3) \quad (4b)$$

$$d_1 = 28.7 - 36.3\hat{\sigma}^{-1} + 42.5\hat{\sigma}^{-2} \quad (5a)$$

$$d_2 = -0.38 + 0.19\hat{\sigma} + 0.03\hat{\sigma}^2 \quad (5b)$$

The extended correlated disorder model (ECDM) can be described as follows [17]:

$$\mu(T, p, E) = [(\mu_{low}(T, p, E))^{q(\hat{\sigma})} + (\mu_{high}(p, E))^{q(\hat{\sigma})}]^{1/q(\hat{\sigma})}, \quad (6)$$

$$q(\hat{\sigma}) = 2.4/(1 - \hat{\sigma}), \quad (7)$$

where  $\mu_{low}(T, p, E)$  and  $\mu_{high}(p, E)$  are the mobility in the low-field limit (the average reduced field  $E_{red} = eaE/\sigma \leq 1$ ) and high-field limit (the average reduced field  $E_{red} = eaE/\sigma \geq 1$ ), respectively.

$$\mu_{low}(T, p, E) = \mu_0(T) g(T, p) f(T, E, p), \quad (8)$$

where  $g(T, p)$  and  $f(T, E, p)$  are the dimensionless mobility enhancement functions. These functions can be written as follows:

$$\mu_0(T) = 1.0 \times 10^{-9} \mu_0 \exp(-0.29\hat{\sigma}^2), \quad (9)$$

$$g(T, p) = \begin{cases} \exp[(0.25\hat{\sigma}^2 + 0.7\hat{\sigma})(2pa^3)^\delta], & pa^3 < 0.025 \\ g(T, 0.025a^{-3}), & pa^3 \geq 0.025 \end{cases}, \quad (10)$$

$$\delta \equiv 2.3 \frac{\ln(0.5\hat{\sigma}^2 + 1.4\hat{\sigma}) - 0.327}{\hat{\sigma}^2}, \quad (11)$$

$$f(T, E_{red}, p) = \exp[h(E_{red})(1.05 - 1.2(pa^3)^{r(\hat{\sigma})}) (\hat{\sigma}^{3/2} - 2)(\sqrt{1 + 2E_{red}} - 1)], \quad (12)$$

$$h(E_{red}) = 1, \quad r(\hat{\sigma}) = 0.7\hat{\sigma}^{-0.7}, \quad (13)$$

within the very low-field,  $0 \leq E_{red} < 0.16 \equiv E_{red}^*$ ,  $h(E_{red})$  can be written as

$$h(E_{red}) = \begin{cases} \frac{4}{3} \frac{E_{red}}{E_{red}^*}, & (E_{red} \leq E_{red}^*/2) \\ \left[1 - \frac{4}{3} \left(\frac{E_{red}}{E_{red}^*} - 1\right)^2\right], & (E_{red}^*/2 \leq E_{red} \leq E_{red}^*) \end{cases}, \quad (14)$$

$$\mu_{high}(p, E) = \frac{2.06 \times 10^{-9}}{E_{red}} \mu_0 (1 - pa^3). \quad (15)$$

By using the above two mobility models, the  $J-V$  characteristics of organic electron devices can be exactly calculated by numerically solving the following equations with a particular uneven discretization method introduced in our previous paper [26, 27].

$$J = p(x)e\mu(T, p(x), E(x))E(x), \quad (16a)$$

$$\frac{dE}{dx} = \frac{e}{\epsilon_0 \epsilon_r} p(x), \quad (16b)$$

$$V = \int_0^L E(x)dx, \quad (16c)$$

where  $x$  is the distance from the injecting electrode,  $L$  is the organic semiconductor layer thickness sandwiched between two electrodes,  $\epsilon_0$  is the vacuum permeability, and  $\epsilon_r$  is the relative dielectric constant of the organic semiconductors.

### 3. Results and discussion

Fig. 1 shows the thickness dependent  $J-V$  characteristics of  $OC_1C_{10}$ -PPV hole-only devices with layer thicknesses of 90 nm and 275 nm at room temperature. Apparently, the experimental  $J-V$  measurements from Ref. [13, 16] can be well described by using the IEGDM in which the mobility depends on the temperature, electric field, and carrier density. The parameters of the width of the Gaussian density of states  $\sigma$ , the intersite distance  $a$ , and  $\mu_0$  are determined in such a way that an optimal overall fit is obtained. Fig. 2 displays the temperature dependent  $J-V$  characteristics of a hole-only device based on  $OC_1C_{10}$ -PPV with a layer thickness of 275 nm. For the entire range of electric field, the temperature dependent hole current could also be accurately described by the IEGDM using the same parameters as the thickness dependent  $J-V$  curves. A clear observation is that the temperature dependent and thickness dependent  $J-V$  characteristics of  $OC_1C_{10}$ -PPV hole-only devices can be excellently described within the IEGDM only using a single set of parameters,  $a = 1.5$  nm,  $\sigma = 0.13$  eV, and  $\mu_0 = 800$  m<sup>2</sup>/Vs. For the model parameters, the value of the disorder parameter  $\sigma$  is close to the value used by Pasveer *et al.* (0.14 eV) [16], and is the same as the result obtained by van Mensfoort *et al.* [28]. The value of intersite distance  $a$  found is very close to the typical value of organic semiconductor [19].

As a next step, we consider the question whether the ECDM can also describe the  $J-V$  characteristics of  $OC_1C_{10}$ -PPV hole-only devices as successfully as the IEGDM. When employing the ECDM, we address the question whether site-energy correlation with this specific correlation function is present in  $OC_1C_{10}$ -PPV. Here, we re-analyse the experimental data from Ref. [13, 16] for  $OC_1C_{10}$ -PPV hole-only devices by employing the ECDM.

In Fig. 3 and Fig. 4, the thickness dependent and temperature dependent  $J-V$  characteristics of  $OC_1C_{10}$ -PPV hole-only devices are displayed, respectively. A clear observation is that the temperature dependent and thickness dependent  $J-V$  characteristics of  $OC_1C_{10}$ -PPV hole-only devices can also be described within the ECDM as successfully as the IEGDM only using a single set of parameters,  $a = 0.2$  nm,  $\sigma = 0.16$  eV, and  $\mu_0 = 1380$  m<sup>2</sup>/Vs.

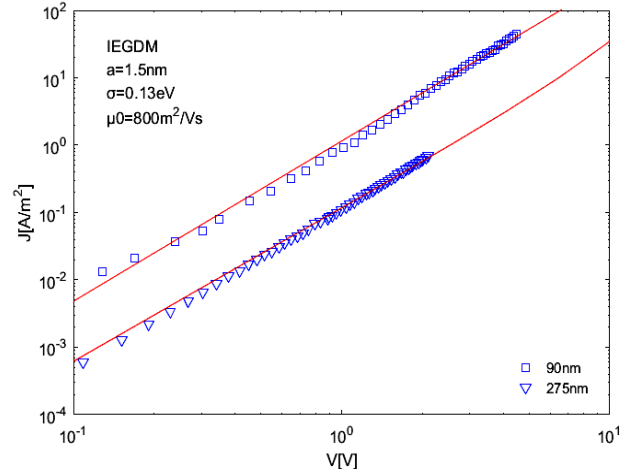


Fig. 1. Thickness dependent  $J-V$  characteristics of  $OC_1C_{10}$ -PPV hole-only devices at room temperature. Symbols are the experimental results from Ref. [13, 16]. Lines are the numerically calculated results based on the IEGDM

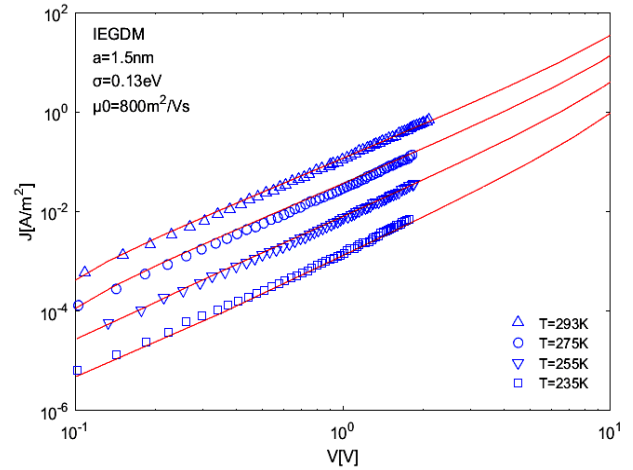


Fig. 2. Temperature dependent  $J-V$  characteristics of  $OC_1C_{10}$ -PPV hole-only device with a layer thickness of 275 nm. Symbols are the experimental results from Ref. [16]. Lines are the numerically calculated results based on the IEGDM

The optimal parameter set for each mobility model is obtained as follows. For a given  $\sigma$ ,  $a$ , and  $\mu_0$  combination, we determine the fitting error between the experimental and calculated  $J-V$  curves for each individual temperature and layer thickness. The total error is calculated as a sum of mean square errors of the fits for

all temperatures and thicknesses. By minimizing this total error, we obtain the optimal model parameter set. Within the IEGDM and ECDM, the carrier density and electric field dependence of the mobility depend only on shape of the Gaussian density of states (DOS), specified by  $\sigma$  and  $a$ . Varying the mobility in the zero-density and zero-field limit, specified by  $\mu_0(T)$ , gives rise to an overall vertical shift of the  $J$ - $V$  curves, but does not affect the shape. It can be clearly seen that within the IEGDM and ECDM the mobility at any temperature and thickness is described by using only three parameters, viz.  $\sigma$ ,  $a$ , and  $\mu_0$ , each parameter has a clear physical meaning. For the IEGDM, the values of  $\sigma$  and  $a$  obtained in this work are 0.13 eV and 1.5 nm, and for the ECDM  $\sigma = 0.16$  eV and  $a = 0.2$  nm. By optimizing the  $J$ - $V$  curves position, the  $\mu_0$  can be determined within two models by using a shift along the vertical axes, 800 and 1380  $\text{m}^2/\text{Vs}$  for the IEGDM and ECDM, respectively.

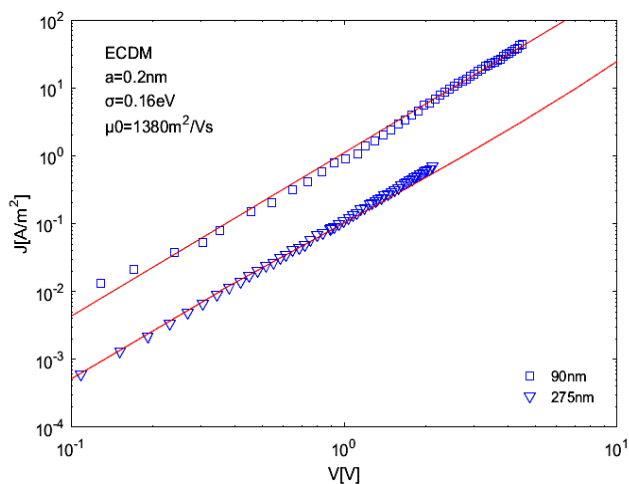


Fig. 3. Thickness dependent  $J$ - $V$  characteristics of  $\text{OC}_1\text{C}_{10}$ -PPV hole-only devices at room temperature. Symbols are the experimental results from Ref. [13, 16]. Lines are the numerically calculated results based on the ECDM

It should be noted that the optimal fit values of  $a$  as obtained from the IEGDM and ECDM are very different, viz. 1.5 nm and 0.2 nm, respectively. The value of  $a$  found for the IEGDM is very close to the typical value of organic semiconductors [19], and slightly smaller than the result reported by Pasveer et al. for  $\text{OC}_1\text{C}_{10}$ -PPV [16]. However, the value of  $a$  found for the ECDM may be considered as unrealistically small, in view of the fact that in  $\text{OC}_1\text{C}_{10}$ -PPV the existence of two asymmetric side chains is expected to give rise to a larger typical distance between neighboring polymer chains. Furthermore, intra-chain hopping between the rather long conjugated segments is also expected to be associated with a larger value of  $a$ . It is generally true that the distance between two subsequent monomer units is approximately 0.7 nm, and the conjugation length is believed to be at least five monomer units. These results suggest that in the

PPV-derivative studied correlation between the site energies is absent or insignificant. The values obtained for  $\sigma$  does not change this point of view. For disordered organic semiconductors, the Gaussian density of states  $\sigma$  is typically observed to fall in the range 0.06-0.16 eV, the optimal values of  $\sigma$  obtained within both models (0.13 eV for the IEGDM and 0.16 eV for the ECDM) are physically realistic. Owing to lack of independent experimental results on the width of the DOS, the values of  $\sigma$  cannot presently be applied to distinguish between the IEGDM and ECDM.

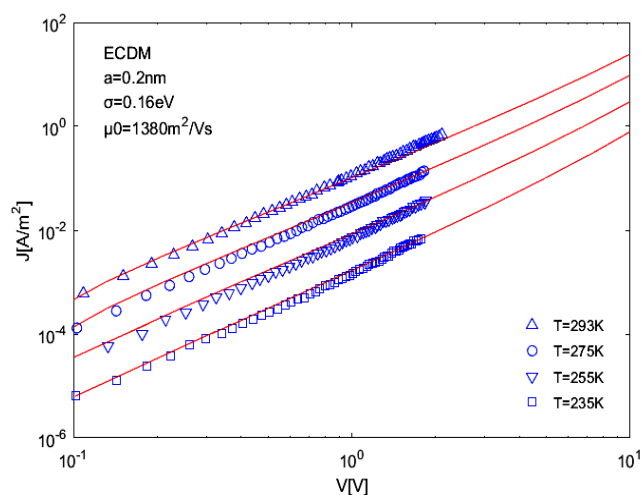


Fig. 4. Temperature dependent  $J$ - $V$  characteristics of  $\text{OC}_1\text{C}_{10}$ -PPV hole-only device with a layer thickness of 275 nm. Symbols are the experimental results from Ref. [16]. Lines are the numerically calculated results based on the ECDM

#### 4. Summary and conclusions

In conclusion, the hole transport in a conjugated PPV-based polymer  $\text{OC}_1\text{C}_{10}$ -PPV has been investigated in the frameworks of the GDM and the CDM while taking the effect of the carrier density dependence of the mobility due to the disorder into account. It is found that excellent and fully consistent descriptions of the thickness dependent and temperature dependent  $J$ - $V$  characteristics of the  $\text{OC}_1\text{C}_{10}$ -PPV hole-only devices can be obtained using the IEGDM and ECDM, within which spatial correlation between the site energies is absent and is included, respectively. An important conclusion is that a successful analysis of the  $J$ - $V$  curves using either model does not yet convincingly prove that the disorder is completely random or correlated. In particular, for the organic material studied, we argue that the most remarkable distinction between the two sets of optimal fit parameters is an observed large difference between the effective intersite distance  $a$ . The more realistic intersite distance is found using the IEGDM ( $a = 1.5$  nm), whereas the value of  $a$  obtained from the ECDM ( $a = 0.2$  nm) may be considered as unrealistically small. We view this

as an indication that for the PPV-derivative studied correlation between the site energies is absent or plays a minor role. Finally, we mention that the parameterizations presented here may be used to investigate the possible role of correlation in other disordered organic semiconductors.

### Acknowledgements

This work is supported by the National Natural Science Foundation of China Grant No. 61501175 and the Doctoral Scientific Research Foundation of Henan Polytechnic University Grant No. B2014-022.

### References

- [1] J. H. Burroughes, D. D. C. Bradley, A. R. Brown, R. N. Marks, K. Mackay, R. H. Friend, P. L. Burns, A. B. Holmes, *Nature* **347**, 539 (1990).
- [2] C. Kasparek, P. W. M. Blom, *Appl. Phys. Lett.* **110**, 023302 (2017).
- [3] A. R. Brown, C. P. Jarrett, D. M. de Leeuw, M. Matters, *Synth. Met.* **88**, 37 (1997).
- [4] B. Kumar, B. K. Kaushik, Y. S. Negi, *Polymer Reviews* **54**, 33 (2014).
- [5] C. J. Brabec, N. S. Sariciftci, J. C. Hummelen, *Adv. Funct. Mater.* **11**, 15 (2001).
- [6] W. Zhao, S. Li, H. Yao, S. Zhang, Y. Zhang, B. Yang, J. Hou, *J. Am. Chem. Soc.* **139**, 148 (2017).
- [7] L. Pautmeier, R. Richert, H. Bässler, *Synth. Met.* **37**, 271 (1990).
- [8] H. Bässler, *Phys. Status Solidi (b)* **175**, 15 (1993).
- [9] Y. Gartstein, E. Conwell, *Chem. Phys. Lett.* **245**, 351 (1995).
- [10] S. V. Novikov, D. H. Dunlap, V. M. Kenkre, P. E. Parris, A. V. Vannikov, *Phys. Rev. Lett.* **81**, 4472 (1998).
- [11] S. Baranovskii, I. Zvyagin, H. Cordes, S. Yamasaki, P. Thomas, *Phys. Status Solidi (b)* **230**, 281 (2002).
- [12] Y. Roichman, N. Tessler, *Synth. Met.* **135**, 443 (2003).
- [13] C. Tanase, P. W. M. Blom, E. J. Meijer, D. M. de Leeuw, *Proc. of SPIE* **5217**, 80 (2003).
- [14] C. Tanase, E. J. Meijer, P. W. M. Blom, D. M. De Leeuw, *Phys. Rev. Lett.* **91**, 216601 (2003).
- [15] R. Coehoorn, W. F. Pasveer, P. A. Bobbert, M. A. J. Michels, *Phys. Rev. B* **72**, 155206 (2005).
- [16] W. F. Pasveer, J. Cottaar, C. Tanase, R. Coehoorn, P. A. Bobbert, P. W. M. Blom, D. M. de Leeuw, M. A. J. Michels, *Phys. Rev. Lett.* **94**, 206601 (2005).
- [17] M. Bouhassoune, S. L. M. van Mensfoort, P. A. Bobbert, R. Coehoorn, *Org. Electron.* **10**, 437 (2009).
- [18] L. G. Wang, H. W. Zhang, X. L. Tang, C. H. Mu, *Eur. Phys. J. B* **74**, 1 (2010).
- [19] L. G. Wang, H. W. Zhang, X. L. Tang, Y. Q. Song, Z. Y. Zhong, Y. X. Li, *Phys. Scr.* **84**, 045701 (2011).
- [20] I. Katsouras, A. Najafi, K. Asadi, A. J. Kronemeijer, A. J. Oostra, L. J. A. Koster, D. M. de Leeuw, P. W. M. Blom, *Org. Electron.* **14**, 1591 (2013).
- [21] L. G. Wang, M. L. Liu, J. J. Zhu, L. F. Cheng, *Optoelectron. Adv. Mat.* **11**(3-4), 202 (2017).
- [22] R. J. de Vries, S. L. M. van Mensfoort, V. Shabro, R. A. J. Janssen, R. Coehoorn, *Appl. Phys. Lett.* **94**, 163307 (2009).
- [23] S. L. M. van Mensfoort, R. J. de Vries, V. Shabro, H. P. Loebel, R. A. J. Janssen, R. Coehoorn, *Org. Electron.* **11**, 1408 (2010).
- [24] S. L. M. van Mensfoort, V. Shabro, R. J. de Vries, R. A. J. Janssen, R. Coehoorn, *J. Appl. Phys.* **107**, 113710 (2010).
- [25] M. L. Liu, L. G. Wang, *J. Optoelectron. Adv. M.* **20**(3-4), 163 (2018).
- [26] L. G. Wang, H. W. Zhang, X. L. Tang, Y. Q. Song, *Optoelectron. Adv. Mat.* **5**(3), 263 (2011).
- [27] M. L. Liu, L. G. Wang, *J. Optoelectron. Adv. M.* **19**(5-6), 406 (2017).
- [28] S. L. M. van Mensfoort, S. I. E. Vulto, R. A. J. Janssen, R. Coehoorn, *Phys. Rev. B* **78**, 085208 (2008).

\*Corresponding author: wangliguo@hpu.edu.cn